

BRANISLAV RAĐENOVIĆ
MARIJA
RADMILOVIĆ-RAĐENOVIĆ

Institute of Physics,
Belgrade, Serbia

SCIENTIFIC WORK

UDC 621.794:661.68:621.38

DOI: 10.2298/HEMIND100205008R

LEVEL SET SIMULATIONS OF THE ANISOTROPIC WET ETCHING PROCESS FOR DEVICE FABRICATION IN NANOTECHNOLOGIES

Chemical etching is employed as micromachining manufacturing process with a purpose of producing micron-size components. As a semiconductor wafer is extremely expensive due to many processing steps involved in the making. The need to critically control the etching end point in an etching process is highly desirable. It was found that not only the etchant and temperature determine the exact anisotropy of etched silicon. It was also shown that the angle between the silicon surface and the mask play an important role. In this paper, angular dependence of the etching rate is calculated on the base of the silicon symmetry properties, by means of the interpolation technique using experimentally obtained values of the principal $\langle 100 \rangle$, $\langle 110 \rangle$, $\langle 111 \rangle$ directions in KOH solutions. The calculations are performed using an extension of the sparse field method for solving three dimensional (3D) level set equations that describe the morphological surface evolution during etching process. The analysis of the obtained results confirmed that, regardless of the initial shape, the profile evolution ends with the crystal form composed of the fastest etching planes, $\{110\}$ in our model.

Etch process is widely used in microfabrication with a purpose of chemically removing layers from the surface of wafer during manufacturing [1–4]. In order to form a functional MEMS structure on a substrate, it is necessary to etch the thin films previously deposited and/or the substrate itself. In general, there are two classes of etching processes. During the, so called, wet etching the material is dissolved when immersed in a chemical solution, while dry etching includes sputtering of the material by using reactive ions or a vapor phase etchant.

Chemical etching process has a long history and was accepted as one of the important nontraditional machining processes during the last half of the century [5]. The method is often applied to machine geometrically complex parts from thin and flat of any material. It is also used to reduce weight of the workpiece materials.

Etching rates and etch end points need to be carefully monitored and controlled in order to end etching processes at the desired time [6,7]. In semiconductor processing, for the semiconductor devices having film layers or features in the micron and sub-micron range, an inadequate etch or an excess etch would lead to insufficient or excess removal of a desired layer. This can cause an undesired open or short electrical circuit connections. Additionally, if the etch is in excess, undercutting or punch through can occur resulting in poorly defined film patterning or total lift-off. Inadequate or excess etching time further leads to undesirable reliability problems in the subsequently fabricated semiconductor device.

Currently, most etch rate end point determination techniques depend on indirect measurement and estimation techniques. Some etch monitoring techniques have

relied on external measurements of film thickness followed by etch rate estimation and an extrapolated etch end point prediction [8,9]. However, etch rates may vary due to batch-to-batch differences in the chemical and physical characteristics of the film or the etchant. Therefore, these extrapolation methods are inadequate.

Previous methods for measuring and minimizing overetch include scanning electron microscopy (SEM) of cross sections of fractured wafers [10]. Not only is the method of analysis destructive to the wafer, there can also be significant imprecision in the resulting estimate of the overetch when the number of sections is insufficient or when the sections are not representative of the whole. Other methods include optical measurements of fiducial regions or discrete test wafers [11]. However, such methods are expensive as portions of the wafer are occupied by non-product fiducial areas or require additional test wafers. Such optical methods are also subject to uncertainty resulting from turbidity of the etch bath and other optical effects and uncertainty resulting from non uniform films. Finally, such optical methods are subject to imprecision in the resulting estimate of overetch when the number of measured sites is insufficient or when the sections are not representative of the whole.

Recently, simulation techniques have evolved into very effective tools that complement laboratory experiments and analytic models [12–15]. Simulation codes have displayed a high level of sophistication and are routinely used in semiconductor industry for predicting various characteristics such as etch rate.

In this paper we discuss the application of the level set method for the modeling of the three dimensional (3D) etching profile evolution during anisotropic wet etching of silicon with KOH etchant [16,17]. Only etching rates along principal directions ($\langle 100 \rangle$, $\langle 110 \rangle$, $\langle 111 \rangle$) of silicon have been considered. Simulation results were achieved by using our simulation package

Corresponding author: M. Radmilović-Rađenović, Institute of Physics, Pregrevica 118, 11080 Belgrade, Serbia.

E-mail: marija@ipb.ac.rs

Paper received: 5 March, 2010

Paper accepted: 16 March, 2010

(well documented in previous publications [18-20]) based on the level set method for the 3D simulation of the etching profile.

RESULTS

Anisotropic wet etching of silicon

Anisotropic wet-chemical etching of silicon in KOH solutions remains the most frequently used processing technique in silicon MEMS technology [21,22]. Very complicated three-dimensional structures can be formed by this technique. In order to simulate the time evolution of three dimensional etching profiles it is essential that exact etch rates in all directions are known. In this paper we shall use etching rate model developed by Hubbard [23]. The etching rates for only a few principal axes are known, but they can be used to determine rate value in an arbitrary direction \mathbf{N} (N_x, N_y, N_z) by an interpolation procedure. It is supposed that N_x, N_y and N_z axes are aligned with $\langle 100 \rangle, \langle 010 \rangle$ and $\langle 001 \rangle$ crystal directions, respectively. In actual calculations we made use of measured etching rates in $\langle 100 \rangle, \langle 110 \rangle$ and $\langle 111 \rangle$ crystal directions, for 30% KOH concentration at 70 °C taken from ref. [16] ($R_{100} = 0.797 \mu\text{m}/\text{min}; R_{110} = 1.455 \mu\text{m}/\text{min}; R_{111} = 0.005 \mu\text{m}/\text{min}$).

The point group of silicon's symmetry $m\bar{3}m$ (subgroup of $Fd\bar{3}m$ space group) contains 48 elements. Since it is not possible to assemble angular section using 3 principal directions with which the whole space can be covered by the symmetry operations, only 16 out of 48 symmetry elements can be used for that purpose. Furthermore, it is necessary to observe only at 1/16th of the full angular extent, that is actually the union of three sections defined by the principal vectors A[100, 111, 110], B[100, 111, 101] and C[001, 111, 101], as depicted in Figure 1.

The etching rate R in an arbitrary direction defined by vector \mathbf{N} is given by an interpolation relation [16]:

$$R(\mathbf{N}) = \begin{cases} \left[R_{100}(N_x - N_y) + R_{110}(N_y - N_z) + R_{111}N_z \right] / N_x; & \mathbf{N} \in A \\ \left[R_{100}(N_x - N_z) + R_{110}(N_z - N_y) + R_{111}N_y \right] / N_x; & \mathbf{N} \in B \\ \left[R_{100}(N_z - N_x) + R_{110}(N_x - N_y) + R_{111}N_y \right] / N_z; & \mathbf{N} \in C \end{cases} \quad (1)$$

Etching rate angular dependence can be obtained by introducing spherical angular coordinates ϕ and θ instead of Cartesian (N_x, N_y, N_z):

$$N_x = \sin \theta \cos \phi; N_y = \sin \theta \sin \phi; N_z = \cos \theta \quad (2)$$

The angular dependence of the etching rate $R(\theta, \phi)$ can be written in the form (and shown as in Figure 2):

$$R(\theta, \phi) = \begin{cases} R_{100} - (R_{110} - R_{111}) \cot \theta / \cos \phi + (R_{110} - R_{100}) \tan \phi; & (\theta, \phi) \in A \\ R_{100} + (R_{110} - R_{100}) \cot \theta / \cos \phi + (R_{111} - R_{110}) \tan \phi; & (\theta, \phi) \in B \\ R_{100} + [(R_{110} - R_{100}) \cos \phi + (R_{110} - R_{100}) \sin \phi] \tan \theta; & (\theta, \phi) \in C \end{cases} \quad (3)$$

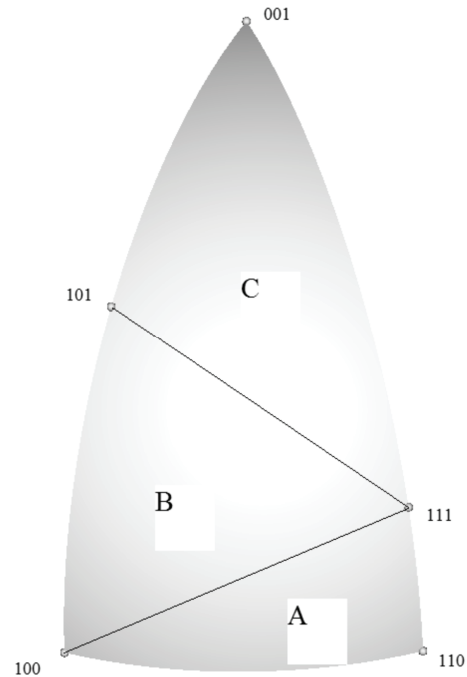


Figure 1. Etching rate model regions used in our 3D simulations.

KOH etching of silicon $\langle 100 \rangle$

Figure 3 displays the etch rates depending on temperature for various solution concentrations (from 20 to 50%). It was found that solutions less than 30% KOH yield rough etching. On the other hand, addition of isopropyl alcohol leads to decreasing of the etch rate by approximately 20%.

Wet etching of silicon ball

In order to demonstrate the strength of the method we have chosen to simulate etching of the silicon ball in KOH etchant also. The initial spherical surface contains all possible velocity directions, so it is expected that the

anisotropy of the etching process will produce the most dramatic changes of the initial shape. This shape is also used in the experimental setup for measuring etching rates anisotropy [18].

In Figure 4 the changes of the initial spherical shape at five equidistant reduced time moments are shown. The influence of the etching rate anisotropy is clearly demon-

strated. During the etching process the initial sphere collapses anisotropically. The etching rate is the smallest in the $\langle 111 \rangle$ directions family and it corresponds to the peaks of the current shape, while the high rate directions $\langle 110 \rangle$ are related to its depths.

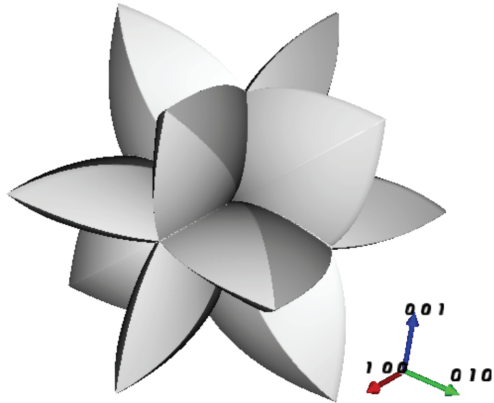


Figure 2. Etching rate angular dependence for 30% KOH concentration at 70 °C.

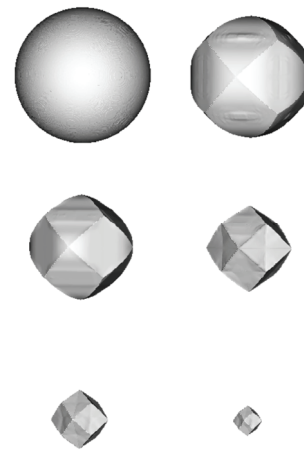


Figure 4. Three-dimensional profile evolution during wet etching of silicon ball.

On the other hand, cube represents the simplest isotropic crystal. The influence of the etching rate anisotropy during the etching of the silicon cube shape made of $\{100\}$ planes is clearly demonstrated in Figure 5. As

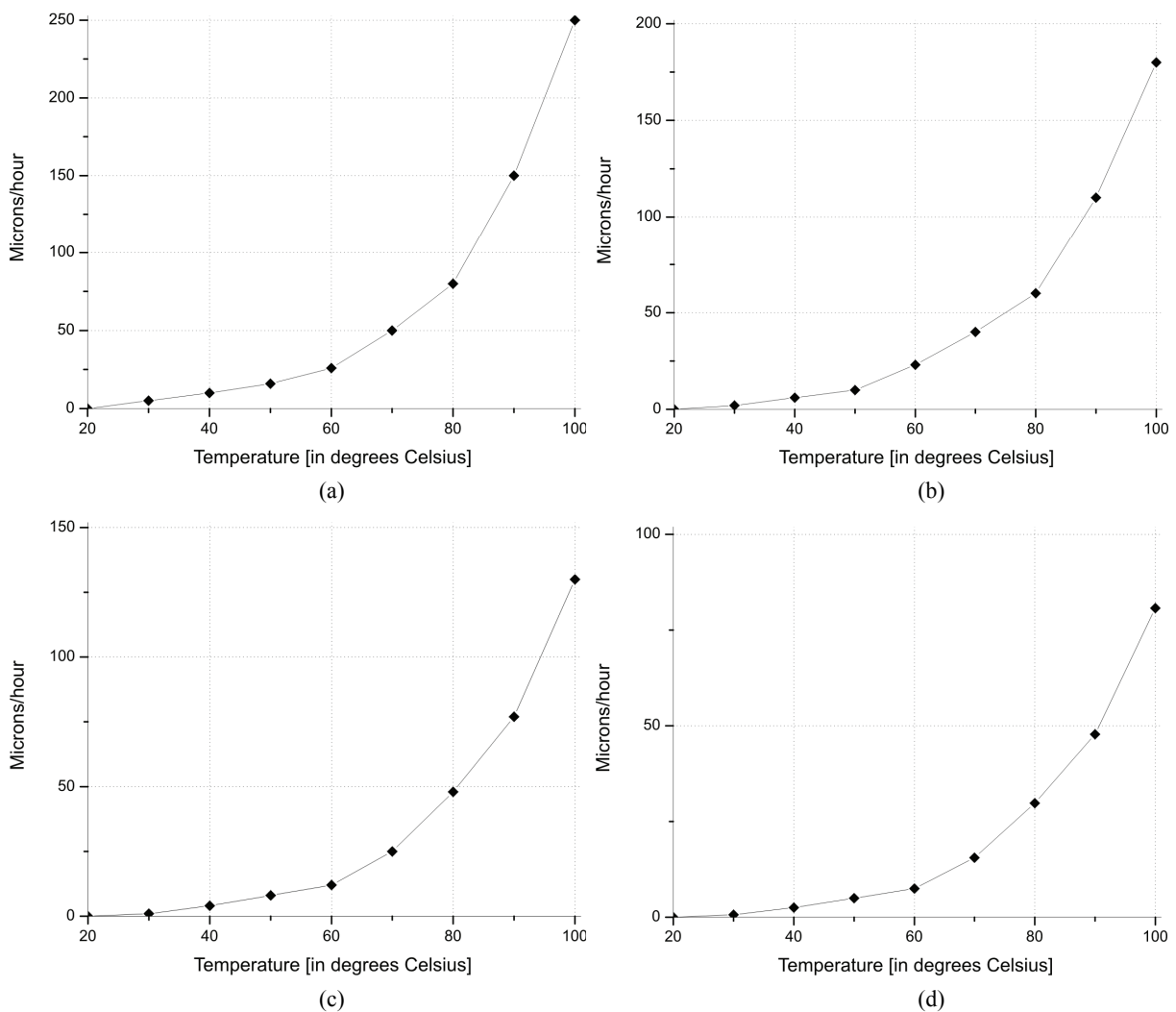


Figure 3. Variation of the KOH etches silicon with the temperature and concentration of the KOH solution: a) 20, b) 40, c) 50 and d) 60%.

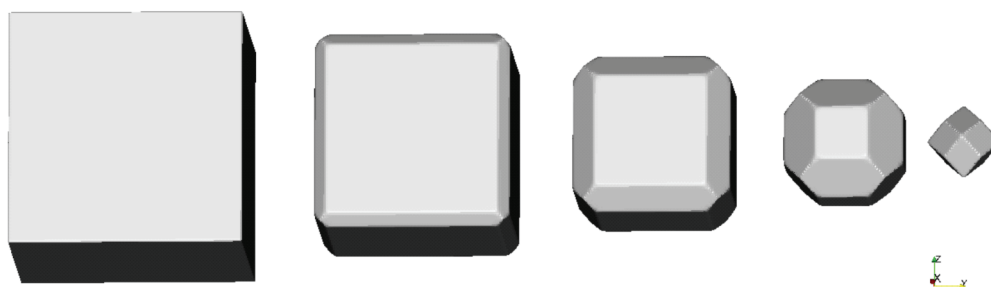


Figure 5. Changes of the initial cubic shape at five equidistant reduced time moments during wet etching.

can be observed, the initial cube shape gradually transforms to the final (rhombic) dodecahedron made of the fastest etching $\{110\}$ principal planes, through the combinations of these shapes. It is expected given that dodecahedron is the only isometric form made of $\{110\}$ planes.

CONCLUSIONS

In this paper we have determined the angular dependence of the etch rates for 30% KOH concentration at 70 °C. The influence of the temperature, as well as the concentration of the KOH solution on the etch rates are also presented. In addition, a 3D simulation of the profile surface evolution during anisotropic wet etching of silicon ball has been performed. This shape is interesting since it contains all possible directions and is used in the experimental setup for measuring etching rates anisotropy. The influence of the etching on the initial cubic shape, as an example of the simplest isometric crystal has been also illustrated. It was shown that inclusion of additional directions for which the etching rates are known, would lead to the better quantitative agreement with the measured data, although it would not cause a visible difference in the figure. The analysis of the obtained results confirm that, regardless of the initial shape, the profile evolution ends with the crystal form composed of the fastest etching planes, $\{110\}$ in our model. Results presented here indicate that the sparse field level set method can be used as an effective tool for wet etching process modeling, and that it is a viable alternative to the cellular automata method, which is today widely used for that purpose [22].

Acknowledgements

The present work has been carried out under the project 141025 of the Ministry of Science and Technological Development of the Republic of Serbia.

REFERENCES

- [1] A. Kumar, G.M. Whitesides, Features of gold having micrometer to centimeter dimensions can be formed though a combination of stamping with an elastomeric stamp and an alkanethiol ink followed by chemical etching. *Appl. Phys. Lett.* **63** (1993) 2002–2004.
- [2] M.J. Madou, *Fundamentals of Microfabrication: The Science of Miniaturization*, 2nd ed., CRC Press, Boca Raton, FL, 2002.
- [3] R. Iosub, C. Moldovan, M. Modreanu, Silicon membranes fabrication by wet anisotropic etching. *Sensor. Actuator. A* **99** (2002) 104–111.
- [4] H. Ni, H.J. Li, A.G. Ramirez, A robust two-step etching process for large-scale microfabricated SiO₂ and Si₃N₄ MEMS membranes. *Sensor. Actuator. A* **119** (2005) 553–558.
- [5] O. Çakır, Chemical etching of aluminium. *J. Mater. Proc. Technol.* **199** (2008) 337–340.
- [6] J.P. Hoekstra, Establishing end point during delineation process. *IBM Technical Disc. Bulletin* **16** (1973) 1717–1720.
- [7] W.M. Goubau, Capacitive etch rate monitor for dielectric etching. *IBM Technical Disc. Bulletin* **31** (1988) 448–449.
- [8] M. Sarfaty, C. Baum, M. Harper, N. Hershkowitz, J.L. Shohet, Real-time monitoring and control of plasma etching. *Jpn. J. Appl. Phys.* **37** (1998) 2381–2387.
- [9] T. Reis, *Advanced Semiconductor Manufacturing Conference, 2001 IEEE/SEMI, Munich, Germany, 2001*, p. 55.
- [10] W. Hu, T. Orlova, G.H. Bernstein, Technique for preparation of precise wafer cross-sections and applications to EBL of PMMA Resist. *J. Vac. Sci. Technol. B* **20** (2002) 3085–3088.
- [11] Z. Xu, S. Li, D.J. Burns, V. Shilpiekandula, H.K. Taylor, S.F. Yoon, K. Youcef-Toumi, I. Reading, Z. Fang, J. Zhao, D.S. Boning, Three-dimensional profile stitching based on the fiducial markers for microfluidic devices. *Opt. Commun.* **282** (2009) 493–499.
- [12] F. Hamaoka, T. Yagisawa, T. Makabe, Modeling of Si etching under effects of plasma molding in two-frequency capacitively coupled plasma in SF₆/O₂ for MEMS fabrication. *IEEE T. Plasma Sci.* **35** (2007) 1350–1358.
- [13] E. Zakka, V. Constantoudis, E. Gogolides, Roughness formation during plasma etching of composite materials: A kinetic Monte Carlo approach. *IEEE T. Plasma Sci.* **35** (2007) 1359–1369.
- [14] J. Van Dijk, G.M.W. Kroesen, A. Bogaerts, Plasma modelling and numerical simulation. *J. Phys. D: Appl. Phys.* **41** (2009) 190301.
- [15] Z.Lj. Petrović, S. Dujko, D. Marić, G. Malović, Ž. Nikitović, O. Šašić, J. Jovanović, V. Stojanović, M. Radmilović-Radenović, Measurement and interpretation of swarm

- parameters and their application in plasma modelling. *J. Phys. D: Appl. Phys.* **42** (2009) 194002.
- [16] K. Sato, M. Shikida, Y. Matsushima, T. Yamashiro, Characterization of orientation dependent etching properties of single crystal silicon: Effect of KOH concentration, *Sensor. Actuator. A* **64** (1988) 87–93.
- [17] I. Zobel, M. Kramkowska, Etch rates and morphology of silicon (*h k l*) surfaces etched in KOH and KOH saturated with isopropanol solutions. *Sensor. Actuator. A* **115** (2004) 549–556.
- [18] B. Radjenović, J.K. Lee, M. Radmilović-Radjenović, Sparse field level set method for non-convex Hamiltonians in 3D plasma etching profile simulations. *Comput. Phys. Commun.* **174** (2006) 127–132.
- [19] B. Radjenović, M. Radmilović-Radjenović, 3D Etching profile evolution simulations: Time dependence analysis of the profile charging during SiO₂ etching in plasma. *J. Phys. Conf. Ser.* **86** (2007) 012017.
- [20] B. Radjenovic, M. Radmilovic-Radjenovic, 3D simulations of the profile evolution during anisotropic wet etching of silicon. *Thin Solid Films* **517** (2009) 4233–4237.
- [21] M. Elwenspoek, H.V. Jansen, *Silicon Micromachining*, Cambridge University Press, Cambridge, UK, 1998.
- [22] M. Gosalvez, K. Sato, A. Foster, R. Nieminen, H. Tanaka, An atomistic introduction to anisotropic etching. *J. Micromech. Microeng.* **17** (2007) S1–S26.
- [23] T.J. Hubbard, *MEMS Design – Geometry of Silicon Micromachining*, Ph.D. Thesis, California Institute of Technology, 1994 (<http://etd.caltech.edu/etd/available/etd-09162005-134646>).

IZVOD

SIMULACIJA PROCESA ANIZOTROPNOG MOKROG NAGRIZANJA METODOM IMPLICITNO DEFINISANIH NIVOVA U NANOTEHNOLOGIJAMA

Branislav Rađenović, Marija Radmilović-Rađenović

Institut za fiziku, Pregrevica 118, 11080 Beograd, Srbija

(Naučni rad)

Hemijsko nagrizanje se koristi u procesu proizvodnje elektronskih komponenti mikronskih dimenzija. S obzirom da je proizvodnja poluprovodničkih supstrata skupa, zbog niza koraka koje je potrebno preduzeti u postupku obrade, precizno određivanje završne tačke kod procesa nagrizanja je od presudne važnosti. Uočeno je da na svojstva rastvora za anizotropno vlažno nagrizanje Si ne utiče samo priroda rastvora i temperatura nagrizanja; ugao između površine Si supstrata i maske takođe igra veoma značajnu ulogu, što je i svojstveno anizotropnom nagrizanju. U ovom radu, ugaona zavisnost brzine nagrizanja je proračunata na osnovu svojstava simetrije Si kristala, interpolacionom tehnikom, koristeći eksperimentalno dobijene vrednosti za brzine nagrizanja u $\langle 100 \rangle$, $\langle 110 \rangle$ i $\langle 111 \rangle$ pravcima iz literature za rastvore KOH. Proračuni su izvršeni koristeći metod retkog polja za rešavanje trodimenzionalnih jednačina implicitno definisanih nivoa koje opisuju morfološki razvoj površine u toku procesa nagrizanja. Analiza dobijenih rezultata potvrđuje da, bez obzira na početni oblik, razvoj profila se završava formom kristala koji se sastoji od ravni sa najvećom brzinom nagrizanja, $\{110\}$ u našem modelu.

Ključne reči: Mokro nagrizanje • Brzina nagrizanja • Nanotehnologija
Key words: Wet etching • Etching rate • Nanotechnology